ATLAS NOTE

ATL-MUON-PUB-2008-006

15 April 2008
revised* 19 May 2008
revised** 23 March 2009
revised*** 4 Dec 2009

ATLAS Muon Chamber Construction Parameters for CSC, MDT, and RPC chambers

Joerg Wotschack (CERN)

Abstract

This paper describes the construction parameters of the Cathode Strip Chambers (CSC), Monitored Drift Tube (MDT) chambers, and the Resistive Plate Chambers (RPC) of the ATLAS Muon Spectrometer.

*) Number of tube layers of EI MDT chambers changed to the correct value of 2×4.
**) Position in z of EEL2A05 and EEL2C05 MDT chambers changed to 10818.5 mm.
***) Spacer height and chamber height of EE MDT chambers changed by 1 mm to 122 mm and 316 mm.

1 The ATLAS Muon spectrometer

The ATLAS muon system is split into two distinct parts: the barrel and the end-caps. In the barrel the muon chambers are arranged in three cylindrical layers around the beam axis that are called BI (Barrel Inner), BM (Barrel Middle), and BO (Barrel Outer). The end-cap chambers are arranged in four disks on each side of the interaction point perpendicular to the beam axis, called EI (End-cap Inner), EE (End-cap Extra), EM (End-cap Middle), and EO (End-cap Outer). An auxiliary set of chambers, called BEE (Barrel End-cap Extra), are installed on the cryostats of the end-cap toroids; they are constructed like barrel chambers although functionally they serve in the end-cap system. Barrel chambers are of rectangular shape and arranged cylindrically around the beam pipe; end-cap chambers are trapezoidal and arranged in planes orthogonal to the beam pipe.

Figure 1 shows a cross-section of the barrel part of the muon system. It illustrates the chamber naming and the numbering of the sectors. The ATLAS co-ordinate system is a right-handed system with the x axis pointing to the centre of the LHC ring, the y axis pointing upwards, and the z axis pointing along the beam axis towards LHC point 8. The azimuthal angle ϕ counts clockwise when looking in the $+z$ direction, the x axis is at $\phi = 0$.

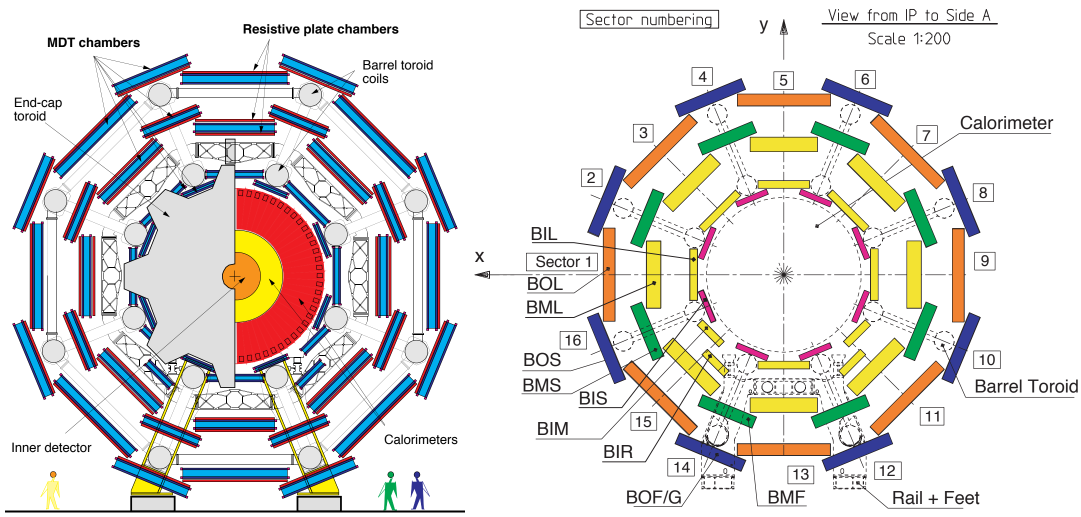

Figure 1: Schematic view of the ATLAS muon spectrometer; cross-section view along the $+z$ direction.

Figures 2 illustrates the naming and the numbering of the muon chambers separately for the odd numbered (top) and even numbered (bottom) sectors. It is is shown for sectors on the A side; the arrangement of chambers on the C side is mirror symmetric to the A side.

Four chamber technologies are employed in the ATLAS muon spectrometer. Monitored Drift Tube (MDT) chambers and Cathode Strip Chambers (CSC) are used for precision measurement; Resistive Plate Chambers (RPC) in the barrel and Thin Gap (multi-wire proportional) Chambers (TGC) in the end-caps for triggering. This paper describes the construction parameters of the first three chamber technologies. The TGCs are described elsewhere.

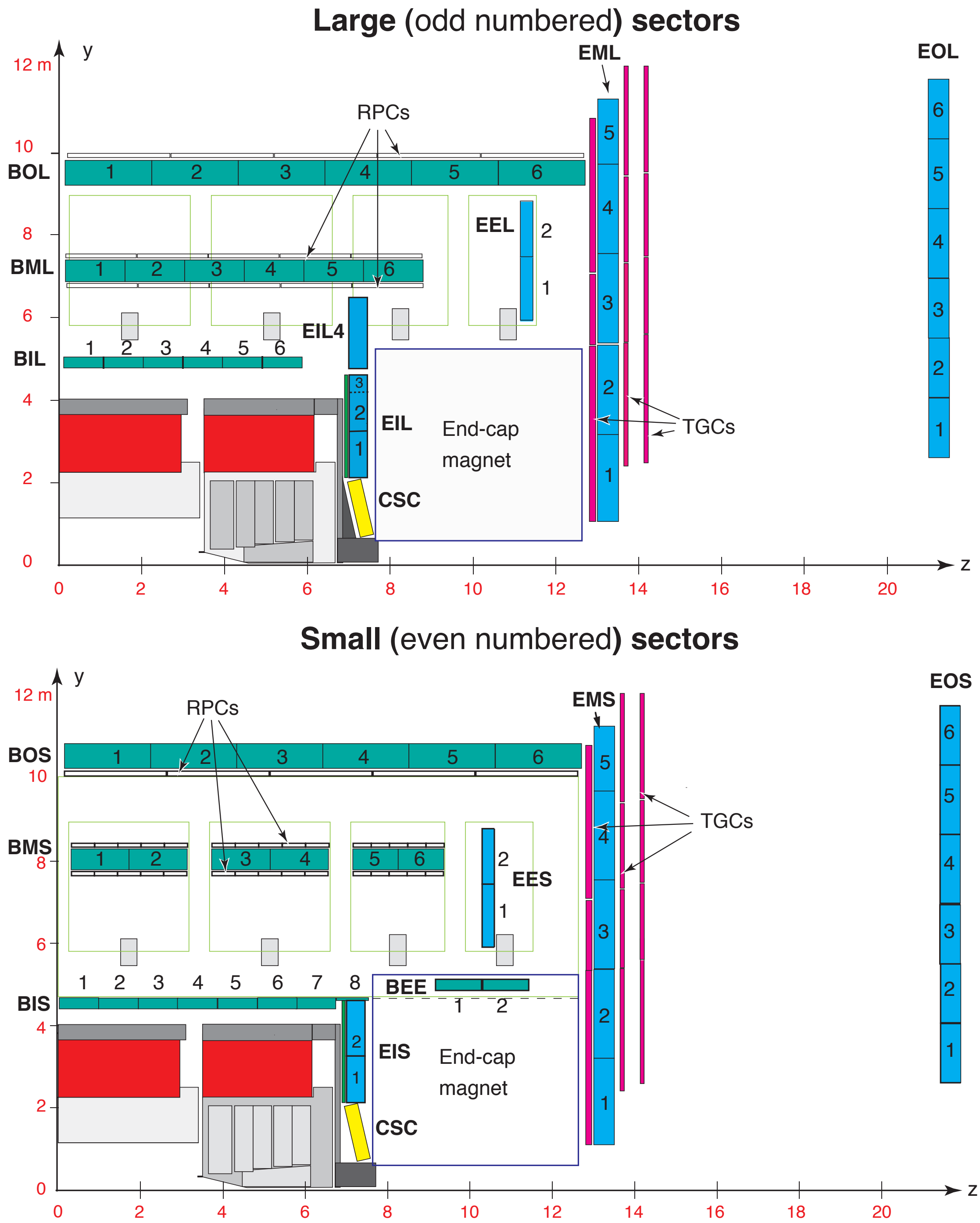

Figure 2: Schematic side view of the ATLAS muon spectrometer depicting the naming and numbering scheme; top: sector with large chambers; bottom: sector with small chambers.

2 MDT system

A description of the MDT chambers can be found in the ATLAS Detector paper. Here a more complete list of construction parameters is collected.

Table 1 gives the overall numbers of elements of the MDT system for the barrel and the end-caps. The main tube parameters and the operational parameters of the MDT chambers are given in Table 2.

Table 1: MDT chambers in numbers. The numbers in brackets refer to the pseudorapidity coverage in the EI plane.

Parameter	Barrel	Endcap	Total
Number of chambers	656	494	1150
Number of tubes	191 568	162 816	354 384
Total wire or tube length (km)	620	463	1083
Chamber area (m^2)	3121	2399	5520
Pseudorapidity coverage	0–1	1–2.7 (2.0)	0–2.7 (2.0)
Chamber weight (t)	129	85	214
Gas volume (m^3)	415	310	725

Table 2: Principal MDT chamber parameters.

Parameter	Value
Tube material	Aluminium (Aluman100)
Outer tube diameter	29.97 mm
Tube wall thickness	0.4 ± 0.020 mm
Wire material	W-Re (97%:3%); 3% gold plating
Wire diameter	50 μm
Wire pitch	30.035 mm
Gas mixture	Ar:CO_2 (93%:7%)
Gas pressure	3 bar (absolute)
Gas gain	2×10^4
Wire potential	3080 V
Maximum drift time	$\sim$750 ns
Average tube resolution	$\sim$75 μm

Figure 3 shows the local chamber coordinate system used in the muon system (here shown for a barrel chamber but the same convention is also used for the end-cap MDTs); the y- and z-axes always point away from the interaction point.

The MDT chambers are installed as shown in Figures 1 and 2; as mentioned above, the arrangement of chambers on the C side is mirror symmetric to the A side. In particular this means that HV and readout ends of the MDTs are for all chambers in a sector on the same side[1]. The general rule is that chambers in even numbered sectors have their HV side at the large-ϕ

[1] The only exception of this rule are the BOG8 chambers in Sector 14, for technical reasons they are installed such that their HV end is on the same side as the readout ends of all other chambers in this sector

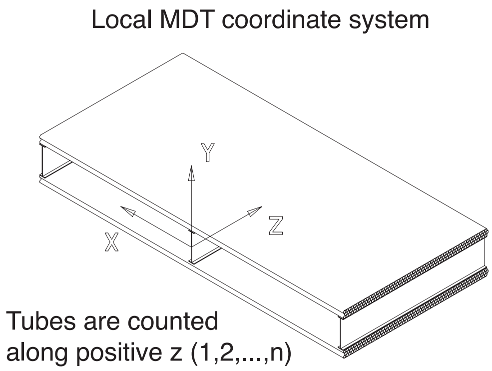

Figure 3: Definition of local chamber coordinate system. The z coordinate of the centre (wire) of the first tube of the chamber is +15 mm.

end and chambers in odd numbered sectors at the small-ϕ end. There are two exceptions: the BOF and BOG chambers in Sector 14 for which the HV end is at low ϕ and the BIL, BIM, and BIR chambers in Sector 11 for which the HV end is at the large-ϕ side.

The parameters describing the individual chambers are given in the following tables. Each chamber family comprises, in general, several chamber types that differ from each other in length (barrel) and/or width (end-cap). In the tables there is one column per type. In the barrel the chamber types are named according to their family and length, e.g. a BIS of 'nomimal length'[2] of 900 mm is called BIS900, etc. In the end-caps the chambers are numbered according to their radial position, e.g., EMS2 is the second EMS chamber when counting from the beam axis.

[2]Nominal length is defined as the number of tubes/layer multiplied by 30 mm; in reality the chambers are longer by half a tube diameter (15 mm) because of the the staggering of the tube layers plus the sum of the additional glue gaps between the tubes.

2.1 Barrel chambers

Table 3 gives the overall numbers of elements of the barrel MDT system. The characteristics and more details of the individual chamber types are given in the following tables.

Table 3: Summary table for the barrel MDTs.

Type	BIS	BIL /M /R	BMS /F	BML	BOS /F /G	BOL	BEE	Total
Number of chambers	128	116	84	94	106	96	32	656
Number of drift tubes	28704	30144	24576	26688	38928	36384	6144	191568
Front-end cards	1196	1270	1024	1112	1664	1516	256	8038

Table 4: Characteristics of BIS chambers; the numbers in brackets refer to sectors 2 and 16.

Construction sites	Beijing (China)	AU Thessaloniki, U and NTU Athens (Greece)	
Type	BIS480	BIS900	BIS1080
Number of chambers	16	90	22
Distance from beam axis (mm)	4620 (4635)	4550 (4635)	4550 (4635)
Chamber length in z (mm)	496.7	916.2	1096.6
Tube length (mm)	851.5	1671.5	1671.5
Tube layers	1×3	2×4	2×4
Tubes/layer	16	30	36
Spacer height (mm)	-	6.5	6.5
Chamber height (mm)	125	284	284
Chamber weight (kg)	20	85	105
Gas volume/chamber (l)	27	269	322
Mezzanine boards/chamber	2	10	12
T-sensors/chamber	3	10	10
B-field sensors/chamber	2	2	2

Table 5: Characteristics of BEE chambers on the end-cap toroid cryostat.

Construction site	Beijing (China)
Type	BEE1440
Number of chambers	32
Distance from beam axis (mm)	4415
Chamber length in z (mm)	1456.7
Tube length (mm)	911.5
Tube layers	1×4
Tubes/layer	48
Spacer height (mm)	-
Chamber height (mm)	170
Chamber weight (kg)	50
Gas volume/chamber (l)	117
Mezzanine boards/chamber	8
T-sensors/chamber	-
B-field sensors/chamber	2

Table 6: Characteristics of BIL chambers; the number in in round brackets refers to the two BIL1 chambers in sectors A09 and C09. The number of B-field sensors mounted on the BIL chambers is not uniform. All BIL1, 3, 5 chambers have 2 sensors, most BIL2, BIL4, and BIL6 chambers carry four sensors, with the exception of BIL2A03 and BIL2A07 that have three sensors only and BIL4A13 and BIL4C13 with two sensors only.

Construction sites	Cosenza, Pavia, Rome I (Italy)		
Type	BIL720	BIL900	BIL1080
Number of chambers	2	37	33
Distance from beam axis (mm)	4949	4949 (5465)	4949
Chamber length in z(mm)	735.8	916.2	1096.6
Tube length (mm)	2671.5	2671.5	2671.5
Tube layers	2×4	2×4	2×4
Tubes/layer	24	30	36
Spacer height (mm)	170	170	170
Chamber height (mm)	416	416	416
Chamber weight (kg)	120	140	160
Gas volume/chamber (l)	343	429	515
Mezzanine boards/chamber	8	10	12
T-sensors/chamber	6	6	6
B-field sensors/chamber	2	2 [4]	4 [2, 3]

Table 7: Characteristics of BIM and BIR chambers; the numbers in brackets refer to the four BIR1 chambers. The BIR720 chambers (BIR5) have only 21 tubes per layer in Multilayer 1; the BIR4 chambers (type BIR900) have only 27 tubes/layer in Multilayer 1.

Construction sites	Cosenza, Pavia, Rome I (Italy)				
Type	BIM1080	BIR720	BIR900	BIR990	BIR1080
Number of chambers	20	4	12	4	4
Distance from beam axis (mm)	5373	6056	6056	6056	6056
Chamber length in z(mm)	1096.6	735.8	916.2	1006.1	1096.6
Tube length (mm)	1536.5	1536.5	1536.5 (2671.5)	1105.5	1105.5
Tube layers	2×4	2×4	2×4	2×4	2×4
Tubes/layer	36	21/24	27/30 (24/30)	33	36
Spacer height (mm)	170	170	170	170	170
Chamber height (mm)	416	416	416	416	416
Chamber weight (kg)	120	85	100 (130)	95	100
Gas volume/chamber (l)	515	185	235 (386)	195	213
Mezzanine boards/chamber	12	8	10	12	12
T-sensors/chamber	6	6	6	6	6
B-field sensors/chamber	1	1	1	-	-

Table 8: Characteristics of BMS and BMF chambers. The numbers in brackets refer to the BMS4 and BMS6 chambers in which the last group of 3×8 tubes in multilayer 1 is missing.

Construction site	JINR Dubna (Russia)				
Type	BMS960	BMS/F1440	BMS1680	BMS/F1920	BMS/F2160
Number of chambers	12	52	12	4	4
Distance from beam axis (mm)	8095	8095	8095	8095	8095
Chamber length in z (mm)	976.1	1456.7	1696.9	1937.2	2177.5
Tube length (mm)	3071.5	3071.5	3071.5	3071.5	3071.5
Tube layers	2×3	2×3	2×3	2×3	2×3
Tubes/layer	32	48 (40)	56	64	72
Spacer height (mm)	170	170	170	170	170
Chamber height (mm)	364	364	364	364	364
Chamber weight (kg)	140	190	215	240	260
Gas volume/chamber (l)	395	592 (543)	691	790	889
Mezzanine boards/chamber	8	12 (11)	14	16	18
T-sensors/chamber	10	10	10	10	10
B-field sensors/chamber	2	2	2	2	2

Table 9: Characteristics of BML chambers.

Construction site	Frascati Nat. Lab. (Italy)			
Type	BML960	BML1200	BML1440	BML1680
Number of chambers	4	35	20	35
Distance from beam axis (mm)	7139	7139	7139	7139
Chamber length in z (mm)	976.1	1216.4	1456.7	1696.9
Tube length (mm)	3551.5	3551.5	3551.5	3551.5
Tube layers	2×3	2×3	2×3	2×3
Tubes/layer	32	40	48	56
Spacer height (mm)	317	317	317	317
Chamber height (mm)	511	511	511	511
Chamber weight (kg)	180	210	240	260
Gas volume/chamber (l)	457	571	685	799
Mezzanine boards/chamber	8	10	12	14
T-sensors/chamber	10	10	10	10
B-field sensors/chamber	-	-	-	-

Table 10: Characteristics of BOS and BOF chambers. The numbers in brackets refer to the BOF chambers (sectors 12 and 14).

Construction sites	LMU and MPI Munich (Germany)			
Type	BOF1200	BOS/F1440	BOS/F1920	BOS/F2160
Number of chambers	4	6	16	62
Distance from beam axis (mm)	10675	10569 (10675)	10569 (10675)	10569 (10675)
Chamber length in z (mm)	1216.4	1456.7	1937.2	2177.5
Tube length (mm)	3773.3	3773.3	3773.3	3773.3
Tube layers	2×3	2×3	2×3	2×3
Tubes/layer	40	48	64	72
Spacer height (mm)	317	317	317	317
Chamber height (mm)	511	511	511	511
Chamber weight (kg)	220	270	300	350
Gas volume/chamber (l)	606	728	970	1092
Mezzanine boards/chamber	10	12	16	18
T-sensors/chamber	18	18	18	18
B-field sensors/chamber	2	2	2	2

Table 11: Characteristics of BOG chambers. These chambers are located inside the detector support feet in sectors 12 and 14; they are T-shaped (except BOG8) and consist of long and short tubes. The dimensions in brackets in the table refer to the first and last six tubes in each tube layer, i.e. 72 tubes out of the 240 total.

Construction site	Freiburg (Germany)	
Type	BOG1200	BOG1200[a]
Number of chambers	14	4
Distance from beam axis (mm)	10675	10675
Chamber length in z (mm)	1216.4	1216.4
Tube length (mm)	3771.5 (1201.5)	3771.5
Tube layers	2×3	2×3
Tubes/layer	28+12[b]	40
Spacer height (mm)	317	317
Chamber height (mm)	511	511
Chamber weight (kg)	200	220
Gas volume/chamber (l)	482	606
Mezzanine boards/chamber	10	10
T-sensors/chamber	28	24
B-field sensors/chamber	2	2

[a]BOG8; these chambers are installed in the last detector support feet on each side of the interaction point; these chambers have no short tubes.

[b]28 long and 12 short tubes

Table 12: Characteristics of BOL chambers.

Construction site	NIKHEF Amsterdam (Netherlands)			
Type	BOL1440	BOL1680	BOL1920	BOL2160
Number of chambers	11	36	1	48
Distance from beam axis (mm)	9500	9500	9500	9500
Chamber length in z (mm)	1456.7	1696.9	1937.2	2177.5
Tube length (mm)	4961.5	4961.5	4961.5	4961.5
Tube layers	2×3	2×3	2×3	2×3
Tubes/layer	48	56	64	72
Spacer height (mm)	317	317	317	317
Chamber height (mm)	511	511	511	511
Chamber weight (kg)	300	340	380	420
Gas volume/chamber (l)	957	1116	1276	1435
Mezzanine boards/chamber	12	14	16	18
T-sensors/chamber	18	18	18	18
B-field sensors/chamber[a]	2	2	2	2

[a]B-field sensors are on all side A chambers, except in sector 13, and on C-side chambers in sectors 5 and 13.

2.2 End-cap chambers

Figure 4 shows the layout of the EI and EE chambers. Figure 5 shows the layout of the EM and EO chambers. The EM chambers are mounted on the movable MDT Big Wheel structures; the EO chambers are fixed and mounted on the HO structures at the two cavern ends.

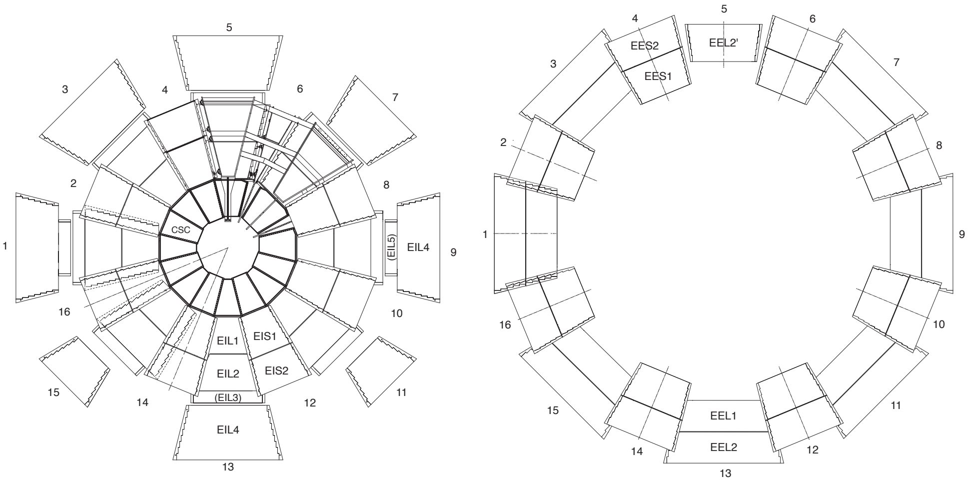

Figure 4: View of the EI (left) and EE (right) chambers from the interaction point onto side A. The EIS chambers of Sector 6 are not drawn to show the Small Wheel support structure.

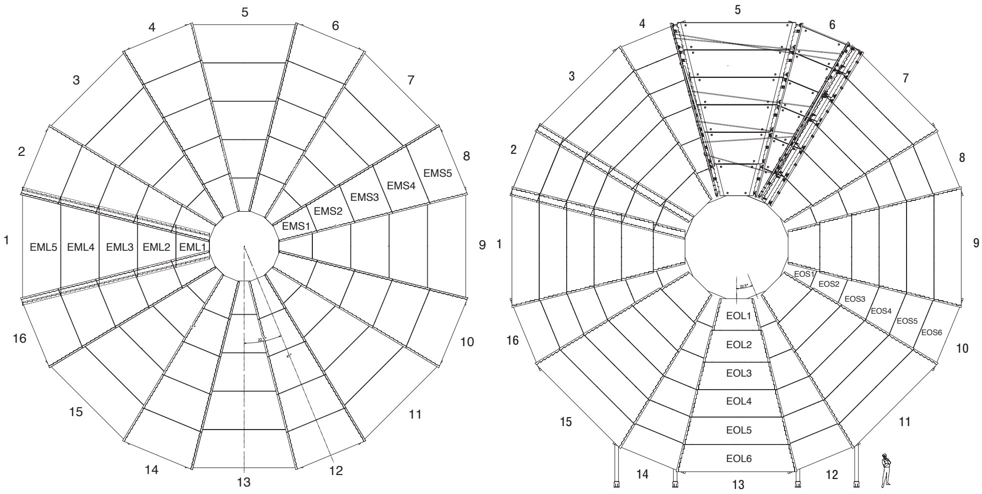

Figure 5: View of the EM (left) and EO (right) chambers from the interaction point onto side A. In Sectors 5 and 6 of the EO chambers the alignment components are shown.

Table 13 gives the overall numbers of elements of the end-cap MDT system. The characteristics and more details of the individual chamber types are given in the following tables.

The parameters of the EI and EE chambers are given in Tables 14, 15, and 16. The parameters of the EM and EO chambers are given in Tables 17, 18, 19, and 20.

Table 13: Summary table for the end-cap MDTs.

Type	EIS	EIL	EES	EEL	EMS	EML	EOS	EOL	Total
Number of chambers	32	48	32	30	80	80	96	96	494
Number of drift tubes	9984	17280	8448	7296	30720	29952	29952	29184	162816
Front-end cards	416	720	352	304	1280	1248	1248	1216	6784

Table 14: Characteristics of EIS and EIL chambers on the Small Wheels.

Construction sites	Boston (USA)					
Type	EIS1	EIS2	EIL1	EIL2	EIL3[a]	
Number of chambers	16	16	16	16	12	4
Distance from beam axis (mm)	2076	3371	2076	3191	4272.3	4272.3
Distance from IP (z mm)	7261	7261	7675	7675	7675	7675
Chamber length in r (mm)	1276.5	1096.2	1096.2	1096.2	375.4	375.4
Tube length min (mm)	898.5	1276.5	1321.5	1861.5	2071.5	1741.5
Tube length max (mm)	1222.5	1546.5	1771.5	2311.5	2071.5	1741.5
Tube layers	2×4	2×4	2×4	2×4	2×4	2×4
Tubes/layer	42	36	36	36	12	12
Spacer height (mm)	121	121	121	121	121	121
Chamber height (mm)	367	367	367	367	367	367
Chamber weight (kg)	140	160	130	190	50	45
Gas volume/chamber (l)	239	272	298	402	133	112
Mezzanine boards/chamber	14	12	12	12	4	4
T-sensors/chamber	8	8	8	8	-	-
B-field sensors/chamber	-	-	-	-	-	-

[a]The EIL3 chambers are rectangular extensions of the EIL2 chambers at large radius; they are not counted as separate chambers but are integral part of the EIL2 chambers and read out together with them.

Table 15: Characteristics of EIL4 chambers; $z = \pm 7641.5$ mm.

Construction sites	Seattle (USA)				Rome I (Italy)
Type (Sectors)	EIL4 (1,9)	EIL4 (3,5,13)	EIL4 (7)	EIL4 (11,15)	EIL5 (1,9)[a]
Number of chambers	4	6	2	4	4
Distance from beam axis (mm)	5080.4	4720	4720	5080.4	4720
Chamber length in r (mm)	1276.5	1636.9	1636.9	1276.5	375.4
Tube length min (mm)	2531.5	2531.5	1651.5	1281.5	1536.5
Tube length max (mm)	3071.5	3071.5	2371.5	1821.5	1536.5
Tube layers	2×4	2×4	2×4	2×4	2×4
Tubes/layer	42	54	54	42	12
Spacer height (mm)	121	121	121	121	121
Chamber height (mm)	367	367	367	367	367
Chamber weight (kg)	190	230	185	140	40
Gas volume/chamber (l)	630	784	582	349	99
Mezzanine boards/chamber	14	18	18	14	4
T-sensors/chamber	20	20	20	20	-
B-field sensors/chamber	4	2	4	4	2

[a]The EIL5 chambers, although built separately, are not counted as separate chambers; they are physically connected to the inner end of and are read out together with the EIL4 chambers, but were constructed separately.

Table 16: Characteristics of EES and EEL chambers.

Construction site	Protvino (Russia)				
Type (Sector)	EES1	EES2	EEL1	EEL2	EEL2 (5)
Number of chambers	16	16	14	14	2
Distance from beam axis (mm)	5893	7370	6513	7749.7	6718
Distance from IP (mm)	10276.5	10276.5	11322.5	11322.5	10818.5
Chamber length in r (mm)	1456.7	1216.4	1216.4	1216.4	1456.7
Tube length min (mm)	2014.5	2446.5	3361.5	3961.5	2446.5
Tube length max (mm)	2374.5	2734.5	3841.5	4441.5	2806.5
Tube layers	2×3	2×3	2×3	2×3	2×3
Tubes/layer	48	40	40	40	48
Spacer height (mm)	122	122	122	122	122
Chamber height (mm)	316	316	316	316	316
Chamber weight (kg)	150	140	170	190	160
Gas volume/chamber (l)	423	416	579	675	507
Mezzanine boards/chamber	12	10	10	10	12
T-sensors/chamber	8	8	8	8	8
B-field sensors/chamber	2	2	-	-	-

Table 17: Characteristics of EMS chambers. All chambers are at a distance of $z = \pm 13878.5$ mm from the interaction point.

Construction sites	Boston (USA)	Seattle (USA)		Michigan (USA)	
Type	EMS1	EMS2	EMS3	EMS4	EMS5
Number of chambers	16	16	16	16	16
Distance from beam axis (mm)	1770	3725	5680	7635	9590
Chamber length in r (mm)	1937.2	1937.2	1937.2	1937.2	1937.2
Tube length min (mm)	835.5	1411.5	1987.5	2563.5	3139.5
Tube length max (mm)	1339.5	1915.5	2491.5	3067.5	3643.5
Tube layers	2×3	2×3	2×3	2×3	2×3
Tubes/layer	64	64	64	64	64
Spacer height (mm)	170	170	170	170	170
Chamber height (mm)	364	364	364	364	364
Chamber weight (kg)	140	180	210	235	260
Gas volume/chamber (l)	280	428	576	724	872
Mezzanine boards/chamber	16	16	16	16	16
T-sensors/chamber	8	20	20	20	20
B-field sensors/chamber	4	2	4	4	2

Table 18: Characteristics of EML chambers. All chambers are at a distance of $z = \pm 14294.5$ mm from the interaction point.

Construction sites	Seattle (USA)		Michigan (USA)		
Type	EML1	EML2	EML3	EML4	EML5
Number of chambers	16	16	16	16	16
Distance from beam axis (mm)	1770	3485	5440	7395	9350
Chamber length in r (mm)	1696.9	1937.2	1937.2	1937.2	1937.2
Tube length min (mm)	1186.5	2026.5	2986.5	3946.5	4906.5
Tube length max (mm)	1906.5	2866.5	3826.5	4786.5	5746.5
Tube layers	2×3	2×3	2×3	2×3	2×3
Tubes/layer	56	64	64	64	64
Spacer height (mm)	170	170	170	170	170
Chamber height (mm)	364	364	364	364	364
Chamber weight (kg)	150	210	250	290	330
Gas volume/chamber (l)	348	629	876	1123	1370
Mezzanine boards/chamber	14	16	16	16	16
T-sensors/chamber	28	20	20	20	20
B-field sensors/chamber	4	4	2	-	-

Table 19: Characteristics of EOS chambers; all chambers are at $z = \pm 21820.5$ mm.

Construction site	Protvino (Russia)					
Type	EOS1	EOS2	EOS3	EOS4	EOS5	EOS6
Number of chambers	16	16	16	16	16	16
Distance from beam axis (mm)	2770	4485	6200	7915	9390	10865
Chamber length in r (mm)	1696.9	1696.9	1696.9	1456.7	1456.7	1456.7
Tube length min (mm)	1249.5	1753.5	2257.5	2761.5	3193.5	3625.5
Tube length max (mm)	1681.5	2185.5	2689.5	3121.5	3553.5	3985.5
Tube layers	2×3	2×3	2×3	2×3	2×3	2×3
Tubes/layer	56	56	56	48	48	48
Spacer height (mm)	170	170	170	170	170	170
Chamber height (mm)	364	364	364	364	364	364
Chamber weight (kg)	140	160	180	180	190	210
Gas volume/chamber (l)	330	443	557	567	651	734
Mezzanine boards/chamber	14	14	14	12	12	12
T-sensors/chamber	8	8	8	8	8	8
B-field sensors/chamber	-	-	-	-	-	-

Table 20: Characteristics of EOL chambers; all chambers are at $z = \pm 21404.5$ mm.

Construction site	Protvino (Russia)					
Type	EOL1	EOL2	EOL3	EOL4	EOL5	EOL6
Number of chambers	16	16	16	16	16	16
Distance from beam axis (mm)	2770	4485	6200	7675	9150	10625
Chamber length in r (mm)	1696.9	1696.9	1456.7	1456.7	1456.7	1456.7
Tube length min (mm)	1681.5	2641.5	3481.5	4201.5	4921.5	5641.5
Tube length max (mm)	2401.5	3361.5	4081.5	4801.5	5521.5	6241.5
Tube layers	2×3	2×3	2×3	2×3	2×3	2×3
Tubes/layer	56	56	48	48	48	48
Spacer height (mm)	170	170	170	170	170	170
Chamber height (mm)	364	364	364	364	364	364
Chamber weight (kg)	170	210	215	235	260	285
Gas volume/chamber (l)	459	675	729	868	1007	1146
Mezzanine boards/chamber	14	14	12	12	12	12
T-sensors/chamber	8	8	8	8	8	8
B-field sensors/chamber	-	-	-	-	-	-

3 CSC system

Cathode strip chambers (CSC) are employed in the ATLAS Muon Spectrometer in the very forward pseudo-rapidiy range (η = 2.0–2.7) in the first end-cap layer. There are 32 CSCs in total, 16 chambers on either detector side. They are installed inclined towards the interaction point by 11.59° with respect to the z axis, see Fig. 6. They come in two versions: small and large CSCs, see Fig. 6.

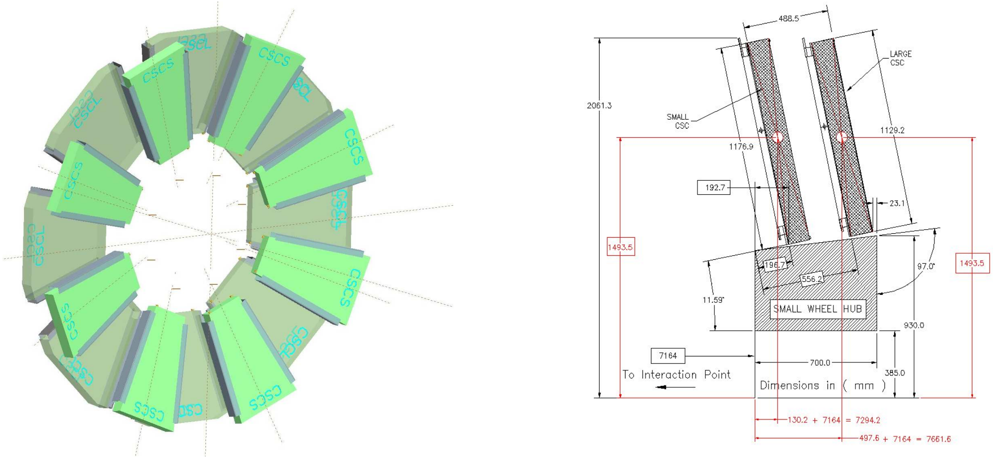

Figure 6: Layout of the CSC chambers; (left) overall view of one side, (right) positions and inclination of the CSCs on the JD shielding hub, note the interaction point is towards the left.

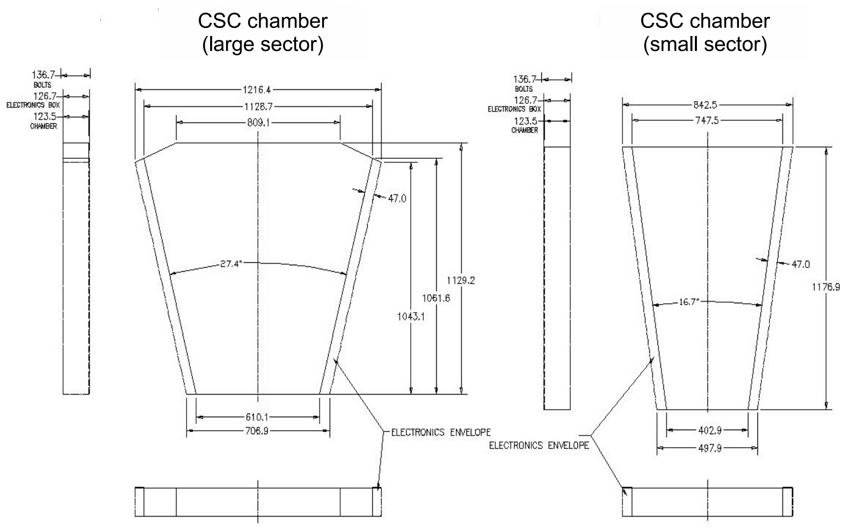

Figure 7: Shapes and dimensions (mm) of the two types of CSC chambers.

The most relevant parameters of the CSCs are given in Tabs 21 and 22.

Table 21: CSC operating parameters.

Parameter	Value
Gas mixture	Ar/CO_2 (80/20)
Operating voltage	1900 V
Gas gain	6×10^4
Number of planes/chamber	4
Anode wire diameter	30μm
Anode wire pitch	2.50 mm
Distance anode wires – cathode strips	2.50 mm

Table 22: CSC chambers in numbers.

Construction site	Brookhaven Nat. Lab. (USA)	
Type	Small	Large
Number of chambers	16	16
Distance[a] from interaction point (mm)	7294	7661
Distance[b] from beam axis (mm)	1493.5	1493.5
Chamber length in r (mm)	1176.9	1129.2
Chamber width (mm)	497.9—747.5	610.1—1126.7
Number of wires/plane	250	402
Number of η strips/plane	574	574
η strip width (mm)	1.602	1.519
η strip gap (mm)	0.250	0.250
Number of η readout strips	192	192
η readout strip pitch (mm)	5.567	5.308
Number of ϕ strips	48	48
ϕ strip width (mm)	12.522	20.604
ϕ strip gap (mm)	0.400	0.400
ϕ readout strip pitch (mm)	12.922	21.004
Active area (m^2)/chamber	0.50	0.78
Gas volume/chamber (l)	107	166
Chamber weight[c] (kg)	70	92
Front-end boards/chamber	10	10

[a]centre of chamber

[b]centre of chamber

[c]total weight, including support frame.

4 RPC system

Resistive plate chambers (RPC) are employed in the ATLAS Muon Spectrometer as trigger chambers in the barrel. They cover the pseudo-rapidiy range (η <1.0) and are arranged in three layers, as shown in Fig. 8. RPC1 and RPC2 are located directly in front and behind the middle barrel chamber MDTs, RPC3 chambers are located in front of the BOS/F MDTs and behind the BOL MDTs. In addition to the RPCs that are assembled together with the MDTs into stations, there are a number of RPCs that are not attached to any MDT. They are located in the middle station and have been introduced to extend the trigger acceptance as much as possible. In the BML layer extra RPC2 chambers (BML7) were added after the BML6 stations; in the BMS layer, 96 small special RPCs were added on both sides of the magnet coil ribs.

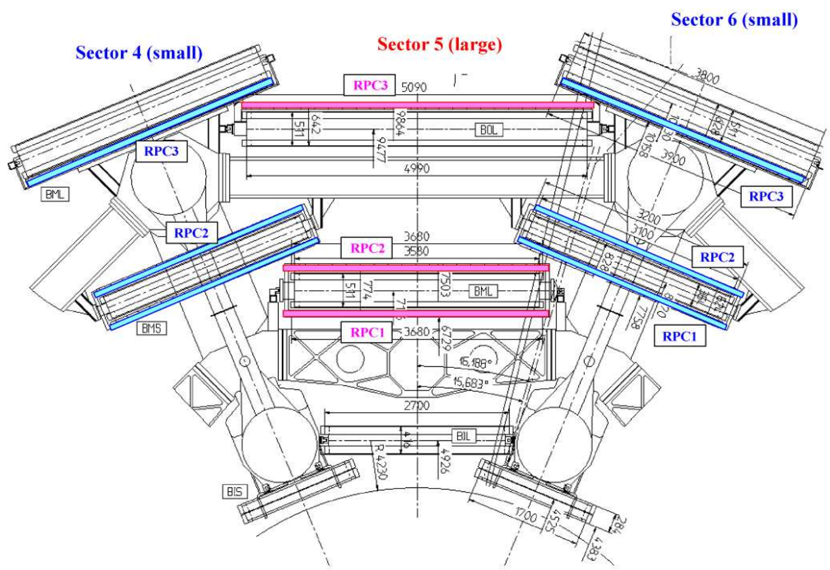

Figure 8: Layout of the standard RPC chambers.

The operating parameters of the RPCs are summarised in Tab. 23

Table 23: RPC operating parameters.

Parameter	Value
Gas mixture	$C_2H_2F_4$/i-C_4H_{10}/SF_6 (94.7/5/0.3)
Operating voltage	4.9 kV/mm
Resistive plate material	Plastic laminate
Resistive plate thickness	1.8 mm
Volume resistivity	10^{10} Ωcm
Surface resistivity of graphite layer	100 kΩ/□
Gas gap thickness	2mm

All RPC units were assembled in the University of Lecce and then tested in the universities of Lecce, Naples, and Rome (University Tor Vergata). The RPC chambers are composed, for the majority of the cases, of two RPC units; for MDT of lengths (z direction) of less than

~1200 mm and for some special cases a single RPC unit forms the chamber. Figure 9 shows the mechanical structure of the RPC units and the way how two RPC units are assembled together to form a chamber, minimising acceptance losses. The overall thickness of the units is 112 mm, this includes some stiffening rib not shown in Fig. 9.

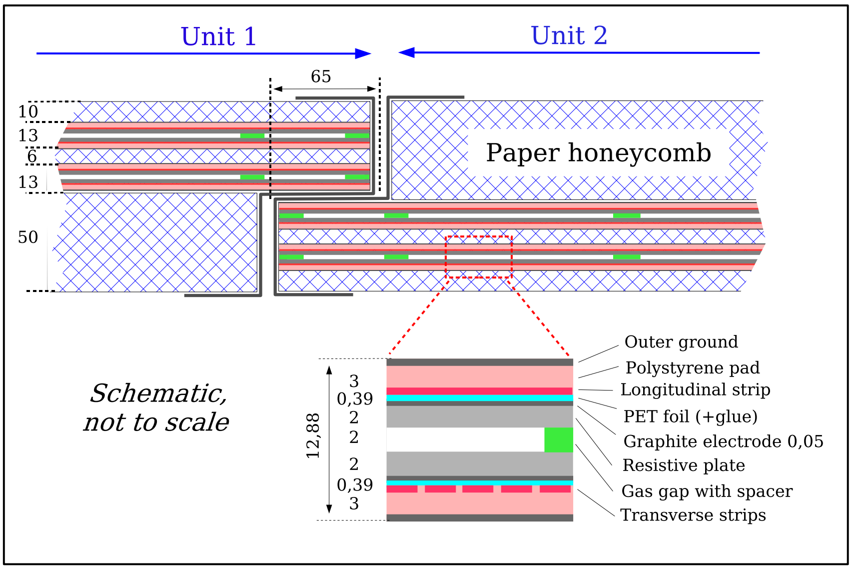

Figure 9: Mechanical structure of the RPC units and the way how two RPC units are assembled together to form a chamber.

The number of units for the different muon stations are summarised in Tab. 24, details for each unit type are given in Tables 25 to 26.

Table 24: Number of RPC units for the different barrel muon stations

Muon station	Number of RPC units
BMS & BMF	296
S1/S2	96
BML	314
BOS, BOF, BOG	218
BOL	192
Total	1116

Tables 25 to 26 give the numbers and dimensions of the different RPC units and their corresponding readout panels.

Table 25: Characteristics of BMS RPC units.

Type	BMS-A[a]	BMS-B	BMS-B⋆	BMS-C	BMS-C⋆	BMS-D[b]	BMS-E[c]
Number of units	8	8	12	16	24	56	176
Unit length in z (mm)	1200	1110	1080	990	960	870	750
Unit width in ϕ (mm)	3200	3200	3200	3200	3200	3200	3200
Active width in ϕ (mm)	2960	2960	2960	2960	2960	2960	2960
Number of layers/unit	2	2	2	2	2	2	2
Number of η strip/layer	80	80	80	64	64	64	48
Pitch of η strips (mm)	29.4	27.2	26.4	30.2	29.3	26.5	30.3
Number of ϕ strip/layer	96	96	96	96	96	96	96
Pitch of ϕ strips (mm)	30.5	30.5	30.5	30.5	30.5	30.5	30.5
Unit area (m^2)	3.6	3.3	3.2	2.9	2.8	2.6	2.2
Unit weight (kg)	132.6	125.6	123.3	114.8	112.4	105.4	94.6
Gas volume/unit (l)	14.2	13.1	12.8	11.7	11.4	10.3	8.9
Front-end boards/unit	44	44	44	40	40	40	36

[a]Four of these units are used for the outer RPC layer of the BOG8 stations.

[b]Four of these units have a cut-out; these are the units closest to the interaction point in RPC1 and RPC2 attached to BMS1A08 and BMS1C08.

[c]12 of these units have a hole for the passage of alignment corridors; these are the units at largest z of the RPC1 chambers attached to the BMS6 MDTs in sectors 02, 04, 06, 08, 10, 16 on side A and C.

Table 26: Characteristics of S2/S3 RPC units.

Type	S2	S3
Number of units	72	24
Unit length in z (mm)	320	660
Unit width in ϕ (mm)	1180	1180
Active width in ϕ (mm)	1060	1060
Number of layers/unit	2	2
Number of η strip/layer	8	24
Pitch of η strips (mm)	37.0	26.5
Number of ϕ strip/layer	32	32
Pitch of ϕ strips (mm)	32.6	32.6
Unit area (m^2)	0.3	0.7
Unit weight (kg)	19.1	31.5
Gas volume/unit (l)	1.4	2.8
Front-end boards/unit	10	14

MDT ch		SIDE A BMS.6	SIDE A BMS.5	Rib	SIDE A BMS.4	SIDE A BMS.3	Rib	SIDE A BMS.2	SIDE A BMS.1	SIDE C BMS.1	SIDE C BMS.2	Rib	SIDE C BMS.3	SIDE C BMS.4	Rib	SIDE C BMS.5	SIDE C BMS.6	
Sector 2		BMS-E | BMS-E	BMS-C*	S2	BMS-E | BMS-E	BMS-E | BMS-E	S2	BMS-E | BMS-E	BMS-D | BMS-D	BMS-D | BMS-D	BMS-E | BMS-E	S2	BMS-E | BMS-E	BMS-E | BMS-E	S2	BMS-C*	BMS-E | BMS-E	RPC2
		1440	960		1440	1440		1440	1680	1680	1440		1440	1440		960	1440	MDT
		BMS-E | BMS-E	BMS-C*	S3	BMS-B*	BMS-E | BMS-E	S2	BMS-E | BMS-E	BMS-D | BMS-D	BMS-D | BMS-D	BMS-E | BMS-E	S2	BMS-E | BMS-E	BMS-B*	S3	BMS-C*	BMS-E | ***BMS-E***	RPC1
Sector 4		BMS-E | BMS-E	BMS-C*	S2	BMS-E | BMS-E	BMS-E | BMS-E	S2	BMS-E | BMS-E	BMS-D | BMS-D	BMS-D | BMS-D	BMS-E | BMS-E	S2	BMS-E | BMS-E	BMS-E | BMS-E	S2	BMS-C*	BMS-E | BMS-E	RPC2
		1440	960		1440	1440		1440	1680	1680	1440		1440	1440		960	1440	MDT
		BMS-E | BMS-E	BMS-C*	S3	BMS-B*	BMS-E | BMS-E	S2	BMS-E | BMS-E	BMS-D | BMS-D	BMS-D | BMS-D	BMS-E | BMS-E	S2	BMS-E | BMS-E	BMS-B*	S3	BMS-C*	BMS-E | ***BMS-E***	RPC1
Sector 6		BMS-E | BMS-E	BMS-C*	S2	BMS-E | BMS-E	BMS-E | BMS-E	S2	BMS-E | BMS-E	BMS-D | BMS-D	BMS-D | BMS-D	BMS-E | BMS-E	S2	BMS-E | BMS-E	BMS-E | BMS-E	S2	BMS-C*	BMS-E | BMS-E	RPC2
		1440	960		1440	1440		1440	1680	1680	1440		1440	1440		960	1440	MDT
		BMS-E | BMS-E	BMS-C*	S3	BMS-B*	BMS-E | BMS-E	S2	BMS-E | BMS-E	BMS-D | BMS-D	BMS-D | BMS-D	BMS-E | BMS-E	S2	BMS-E | BMS-E	BMS-B*	S3	BMS-C*	BMS-E | ***BMS-E***	RPC1
Sector 8		BMS-E | BMS-E	BMS-C*	S2	BMS-E | BMS-E	BMS-E | BMS-E	S2	BMS-E | BMS-E	BMS-D | ***BMS-D***	***BMS-D*** | BMS-D	BMS-E | BMS-E	S2	BMS-E | BMS-E	BMS-E | BMS-E	S2	BMS-C*	BMS-E | BMS-E	RPC2
		1440	960		1440	1440		1440	1680	1680	1440		1440	1440		960	1440	MDT
		BMS-E | BMS-E	BMS-C*	S3	BMS-B*	BMS-E | BMS-E	S2	BMS-E | BMS-E	BMS-D | ***BMS-D***	***BMS-D*** | BMS-D	BMS-E | BMS-E	S2	BMS-E | BMS-E	BMS-B*	S3	BMS-C*	BMS-E | ***BMS-E***	RPC1
Sector 10		BMS-E | BMS-E	BMS-C*	S2	BMS-E | BMS-E	BMS-E | BMS-E	S2	BMS-E | BMS-E	BMS-D | BMS-D	BMS-D | BMS-D	BMS-E | BMS-E	S2	BMS-E | BMS-E	BMS-E | BMS-E	S2	BMS-C*	BMS-E | BMS-E	RPC2
		1440	960		1440	1440		1440	1680	1680	1440		1440	1440		960	1440	MDT
		BMS-E | BMS-E	BMS-C*	S3	BMS-B*	BMS-E | BMS-E	S2	BMS-E | BMS-E	BMS-D | BMS-D	BMS-D | BMS-D	BMS-E | BMS-E	S2	BMS-E | BMS-E	BMS-B*	S3	BMS-C*	BMS-E | ***BMS-E***	RPC1
Sector 16		BMS-E | BMS-E	BMS-C*	S2	BMS-E | BMS-E	BMS-E | BMS-E	S2	BMS-E | BMS-E	BMS-D | BMS-D	BMS-D | BMS-D	BMS-E | BMS-E	S2	BMS-E | BMS-E	BMS-E | BMS-E	S2	BMS-C*	BMS-E | BMS-E	RPC2
		1440	960		1440	1440		1440	1680	1680	1440		1440	1440		960	1440	MDT
		BMS-E | BMS-E	BMS-C*	S3	BMS-B*	BMS-E | BMS-E	S2	BMS-E | BMS-E	BMS-D | BMS-D	BMS-D | BMS-D	BMS-E | BMS-E	S2	BMS-E | BMS-E	BMS-B*	S3	BMS-C*	BMS-E | ***BMS-E***	RPC1

MDT ch	*Foot*	SIDE A	*Foot*	SIDE A BMF3	*Foot*	SIDE A BMF2	*Foot*	SIDE A BMF1	*Foot*	SIDE C BMF1	*Foot*	SIDE C BMF2	*Foot*	SIDE C BMF3	*Foot*	SIDE C	*Foot*
Sector 12		Empty		BMS-E | BMS-E		BMS-C | BMS-C		BMS-B | BMS-B		BMS-B | BMS-B		BMS-C | BMS-C		BMS-E | BMS-E		Empty	
				1440		1920		2160		2160		1920		1440			
				BMS-A		BMS-D | BMS-D		BMS-C | BMS-C		BMS-C | BMS-C		BMS-D | BMS-D		BMS-A			
Sector 14		Empty		BMS-E | BMS-E		BMS-C | BMS-C		BMS-B | BMS-B		BMS-B | BMS-B		BMS-C | BMS-C		BMS-E | BMS-E		Empty	
				1440		1920		2160		2160		1920		1440			
				BMS-A		BMS-D | BMS-D		BMS-C | BMS-C		BMS-C | BMS-C		BMS-D | BMS-D		BMS-A			

Figure 10: Assignment of the BMS and BMF RPC units to the muon stations.

Table 27: Characteristics of BML RPC units.

Type	BML-A	BML-D	BML-E	BML-G$^{\star a}$
Number of units	70	148	80	16
Unit length in z (mm)	1200	870	750	480
Unit width in ϕ (mm)	3680	3680	3680	3280
Active width in ϕ (mm)	3440	3440	3440	3040
Number of layers/unit	2	2	2	2
Number of η strip/layer	80	64	48	32
Pitch of η strips (mm)	29.4	26.5	30.3	28.5
Number of ϕ strip/layer	128	128	128	112
Pitch of ϕ strips (mm)	26.6	26.6	26.6	26.8
Unit area (m^2)	4.1	3.0	2.6	1.5
Unit weight (kg)	150.3	119.1	106.7	73.7
Gas volume/unit (l)	16.5	12.0	10.3	5.8
Front-end boards/unit	52	48	44	36

[a] single RPC2 chambers of BML7

		SIDE A						SIDE C						
MDT ch		BML6	BML5	BML4	BML3	BML2	BML1	BML1	BML2	BML3	BML4	BML5	BML6	
Sector 1	BML-G	BML-E BML-E	BML-A	BML-A	BML-D BML-D	BML-D BML-D	BML-D BML-D	BML-D	BML-D BML-D	BML-D BML-D	BML-A	BML-A	BML-E BML-E	BML-G
		1440	1200	1200	1680	1680	1680	960	1680	1680	1200	1200	1440	
		BML-E BML-E	BML-A	BML-A	BML-D BML-D	BML-D BML-D	BML-D BML-D	BML-D	BML-D BML-D	BML-D BML-D	BML-A	BML-A	BML-E BML-E	
Sector 3	BML-G	BML-E BML-E	BML-A	BML-A	BML-D BML-D	BML-D BML-D	BML-D BML-D	BML-E BML-E	BML-D BML-D	BML-D BML-D	BML-A	BML-A	BML-E BML-E	BML-G
		1440	1200	1200	1680	1680	1680	1440	1680	1680	1200	1200	1440	
		BML-E BML-E	BML-A	BML-A	BML-D BML-D	BML-D BML-D	BML-D BML-D	BML-E BML-E	BML-D BML-D	BML-D BML-D	BML-A	BML-A	BML-E BML-E	
Sector 5	BML-G	BML-E BML-E	BML-A	BML-A	BML-D BML-D	BML-D BML-D	BML-E BML-E	BML-E BML-E	BML-D BML-D	BML-D BML-D	BML-A	BML-A	BML-E BML-E	BML-G
		1440	1200	1200	1680	1680	1440	1440	1680	1680	1200	1200	1440	
		BML-E BML-E	BML-A	BML-A	BML-D BML-D	BML-D BML-D	BML-E BML-E	BML-E BML-E	BML-D BML-D	BML-D BML-D	BML-A	BML-A	BML-E BML-E	
Sector 7	BML-G	BML-E BML-E	BML-A	BML-A	BML-D BML-D	BML-D BML-D	BML-D	BML-D	BML-D BML-D	BML-D BML-D	BML-A	BML-A	BML-E BML-E	BML-G
		1440	1200	1200	1680	1680	960	960	1680	1680	1200	1200	1440	
		BML-E BML-E	BML-A	BML-A	BML-D BML-D	BML-D BML-D	BML-D	BML-D	BML-D BML-D	BML-D BML-D	BML-A	BML-A	BML-E BML-E	
Sector 9	BML-G	BML-E BML-E	BML-A	BML-A	BML-D BML-D	BML-D BML-D	BML-D	BML-A	BML-D BML-D	BML-D BML-D	BML-A	BML-A	BML-E BML-E	BML-G
		1440	1200	1200	1680	1680	960	1200	1680	1680	1200	1200	1440	
		BML-E BML-E	BML-A	BML-A	BML-D BML-D	BML-D BML-D	BML-D	BML-A	BML-D BML-D	BML-D BML-D	BML-A	BML-A	BML-E BML-E	
Sector 11	BML-G	BML-E BML-E	BML-A	BML-A	BML-D BML-D	BML-D BML-D	BML-A	BML-A	BML-D BML-D	BML-D BML-D	BML-A	BML-A	BML-E BML-E	BML-G
		1440	1200	1200	1680	1680	1200	1200	1680	1680	1200	1200	1440	
		BML-E BML-E	BML-A	BML-A	BML-D BML-D	BML-D BML-D	BML-A	BML-A	BML-D BML-D	BML-D BML-D	BML-A	BML-A	BML-E BML-E	
Sector 13	BML-G	BML-E BML-E	BML-A	Elevator	BML-D BML-D	BML-D BML-D	BML-E BML-E	BML-D BML-D	BML-D BML-D	BML-D BML-D	Elevator	BML-A	BML-E BML-E	BML-G
		1440	1200		1680	1680	1440	1680	1680	1680		1200	1440	
		BML-E BML-E	BML-A		BML-D BML-D	BML-D BML-D	BML-E BML-E	BML-D BML-D	BML-D BML-D	BML-D BML-D		BML-A	BML-E BML-E	
Sector 15	BML-G	BML-E BML-E	BML-A	BML-A	BML-D BML-D	BML-D BML-D	BML-A	BML-A	BML-D BML-D	BML-D BML-D	BML-A	BML-A	BML-E BML-E	BML-G
		1440	1200	1200	1680	1680	1200	1200	1680	1680	1200	1200	1440	
		BML-E BML-E	BML-A	BML-A	BML-D BML-D	BML-D BML-D	BML-A	BML-A	BML-D BML-D	BML-D BML-D	BML-A	BML-A	BML-E BML-E	

Figure 11: Assignment of the BML RPC units to the muon stations.

Table 28: Characteristics of BOS RPC units.

Type	BOS-A[a]	BOS-B[b]	BOS-C	BOS-D	BOS-D*	BOS-E
Number of units	12	136	16	12	18	20
Unit length in z (mm)	1200	1110	990	870	840	750
Unit width in ϕ (mm)	3900	3900	3900	3900	3900	3900
Active width in ϕ (mm)	3660	3660	3660	3660	3660	3660
Number of layers/unit	2	2	2	2	2	2
Number of η strip/layer	80	64	64	64	64	48
Pitch of η strips (mm)	29.4	34.0	30.2	26.5	26.5	30.3
Number of ϕ strip/layer	128	128	128	128	128	128
Pitch of ϕ strips (mm)	28.3	28.3	28.3	28.3	28.3	28.3
Unit area (m^2)	4.4	4.1	3.6	3.2	3.1	2.7
Unit weight (kg)	132.6	125.6	123.3	114.8	109.4	112.4
Gas volume/unit (l)	17.4	16.3	14.5	12.7	12.3	11.0
Front-end boards/unit	52	48	48	48	48	36

[a] Four of these units have holes for the passage of alignment corridors; these are the units forming RPC3 of the BOG8A12, BOG8C12, BOG8A14, BOG8C14.

[b] 12 of these units have a hole for the passage of alignment corridors; these are the units at small z of the RPC3 chambers attached to the BOS6 MDTs in sectors 02, 04, 06, 08, 10, 16 on side A and C, the holes on side A and C are mirror symmetric, i.e. units on side A and C are different.

SIDE A

MDT ch	BOS6	BOS5	BOS4	BOS3	BOS2	BOS1
Sector 2	1920 BOS-D | ***BOS-B***	2160 BOS-B | BOS-B	2160 BOS-B | BOS-B	2160 BOS-B | BOS-B	2160 BOS-B | BOS-B	2160 BOS-B | BOS-B
Sector 4	1920 BOS-D | ***BOS-B***	2160 BOS-B | BOS-B	2160 BOS-B | BOS-B	2160 BOS-B | BOS-B	2160 BOS-B | BOS-B	2160 BOS-B | BOS-B
Sector 6	1920 BOS-D | ***BOS-B***	2160 BOS-B | BOS-B	2160 BOS-B | BOS-B	2160 BOS-B | BOS-B	2160 BOS-B | BOS-B	2160 BOS-B | BOS-B
Sector 8	1920 BOS-D | ***BOS-B***	2160 BOS-B | BOS-B	2160 BOS-B | BOS-B	2160 BOS-B | BOS-B	2160 BOS-B | BOS-B	1440 BOS-E | BOS-E
Sector 10	1920 BOS-D | ***BOS-B***	2160 BOS-B | BOS-B	2160 BOS-B | BOS-B	2160 BOS-B | BOS-B	2160 BOS-B | BOS-B	2160 BOS-B | BOS-B
Sector 16	1920 BOS-D | ***BOS-B***	2160 BOS-B | BOS-B	2160 BOS-B | BOS-B	2160 BOS-B | BOS-B	2160 BOS-B | BOS-B	2160 BOS-B | BOS-B

SIDE C

MDT ch	BOS1	BOS2	BOS3	BOS4	BOS5	BOS6
Sector 2	2160 BOS-B | BOS-B	2160 BOS-B | BOS-B	2160 BOS-B | BOS-B	2160 BOS-B | BOS-B	2160 BOS-B | BOS-B	1920 ***BOS-B*** | BOS-D
Sector 4	2160 BOS-B | BOS-B	2160 BOS-B | BOS-B	2160 BOS-B | BOS-B	2160 BOS-B | BOS-B	2160 BOS-B | BOS-B	1920 ***BOS-B*** | BOS-D
Sector 6	2160 BOS-B | BOS-B	2160 BOS-B | BOS-B	2160 BOS-B | BOS-B	2160 BOS-B | BOS-B	2160 BOS-B | BOS-B	1920 ***BOS-B*** | BOS-D
Sector 8	1440 BOS-E | BOS-E	2160 BOS-B | BOS-B	2160 BOS-B | BOS-B	2160 BOS-B | BOS-B	2160 BOS-B | BOS-B	1920 ***BOS-B*** | BOS-D
Sector 10	2160 BOS-B | BOS-B	2160 BOS-B | BOS-B	2160 BOS-B | BOS-B	2160 BOS-B | BOS-B	2160 BOS-B | BOS-B	1920 ***BOS-B*** | BOS-D
Sector 16	2160 BOS-B | BOS-B	2160 BOS-B | BOS-B	2160 BOS-B | BOS-B	2160 BOS-B | BOS-B	2160 BOS-B | BOS-B	1920 ***BOS-B*** | BOS-D

SIDE A

	Foot		*Foot*		*Foot*		*Foot*		*Foot*
MDT ch	BOG8	BOF7	*BOG6*	BOF5	*BOG4*	BOF3	*BOG2*	BOF1	*BOG0*
Sector 12	BMS-E 1200 ***BOS-A***	BOS-A 1200 BOS-A	BOS-D* 1200 BOS-D*	BOS-E | BOS-E 1440 BOS-E | BOS-E	1200 BOS-D*	BOS-C | BOS-C 1920 BOS-C | BOS-C	1200 BOS-D*	2160 BOS-B | BOS-B	1200 BOS-D*
Sector 14	BMS-E 1200 ***BOS-A***	BOS-A 1200 BOS-A	BOS-D* 1200 BOS-D*	BOS-E | BOS-E 1440 BOS-E | BOS-E	1200 BOS-D*	BOS-C | BOS-C 1920 BOS-C | BOS-C	1200 BOS-D*	2160 BOS-B | BOS-B	1200 BOS-D*

SIDE C

		Foot		*Foot*		*Foot*		*Foot*
MDT ch	BOF1	*BOG2*	BOF3	*BOG4*	BOF5	*BOG6*	BOF7	BOG8
Sector 12	2160 BOS-B | BOS-B	1200 BOS-D*	BOS-C | BOS-C 1920 BOS-C | BOS-C	1200 BOS-D*	BOS-E | BOS-E 1440 BOS-E | BOS-E	BOS-D* 1200 BOS-D*	BOS-A 1200 BOS-A	BMS-E 1200 ***BOS-A***
Sector 14	2160 BOS-B | BOS-B	1200 BOS-D*	BOS-C | BOS-C 1920 BOS-C | BOS-C	1200 BOS-D*	BOS-E | BOS-E 1440 BOS-E | BOS-E	BOS-D* 1200 BOS-D*	BOS-A 1200 BOS-A	BMS-E 1200 ***BOS-A***

Figure 12: Assignment of the BOS, BOF, and BOG RPC units to the muon stations.

Table 29: Characteristics of BOL RPC units.

Type	BOL-B	BOL-D	BOL-E
Number of units	97	73	22
Unit length in z (mm)	1110	870	750
Unit width in ϕ (mm)	5090	5090	5090
Active width in ϕ (mm)	4850	4850	4850
Number of layers/unit	2	2	2
Number of η strip/layer	64	48	48
Pitch of η strips (mm)	34.0	35.3	30.3
Number of ϕ strip/layer	160	160	160
Pitch of ϕ strips (mm)	30.1	30.1	30.1
Unit area (m^2)	5.4	4.2	3.6
Unit weight (kg)	186.4	155.1	140.5
Gas volume/unit (l)	21.5	16.9	14.6
Front-end boards/unit	56	52	52

	SIDE A						SIDE C					
MDT ch	BOL6	BOL5	BOL4	BOL3	BOL2	BOL1	BOL1	BOL2	BOL3	BOL4	BOL5	BOL6
Sector 1	BOL-D BOL-D 1680	BOL-B BOL-B 2160	BOL-B BOL-B 2160	BOL-D BOL-D 1680	BOL-B BOL-B 2160	BOL-B BOL-B 2160	BOL-E BOL-E 1440	BOL-B BOL-B 2160	BOL-D BOL-D 1680	BOL-B BOL-B 2160	BOL-B BOL-B 2160	BOL-D BOL-D 1680
Sector 3	BOL-D BOL-D 1680	BOL-B BOL-B 2160	BOL-B BOL-B 2160	BOL-D BOL-D 1680	BOL-B BOL-B 2160	BOL-B BOL-B 2160	BOL-E BOL-E 1440	BOL-B BOL-B 2160	BOL-D BOL-D 1680	BOL-B BOL-B 2160	BOL-B BOL-B 2160	BOL-D BOL-D 1680
Sector 5	BOL-D BOL-D 1680	BOL-B BOL-B 2160	BOL-B BOL-B 2160	BOL-D BOL-D 1680	BOL-B BOL-B 2160	BOL-B BOL-D 1920	BOL-E BOL-E 1440	BOL-E BOL-E 1440	BOL-D BOL-D 1680	BOL-B BOL-B 2160	BOL-B BOL-B 2160	BOL-D BOL-D 1680
Sector 7	BOL-D BOL-D 1680	BOL-B BOL-B 2160	BOL-B BOL-B 2160	BOL-D BOL-D 1680	BOL-B BOL-B 2160	BOL-E BOL-E 1440	BOL-E BOL-E 1440	BOL-B BOL-B 2160	BOL-D BOL-D 1680	BOL-B BOL-B 2160	BOL-B BOL-B 2160	BOL-D BOL-D 1680
Sector 9	BOL-D BOL-D 1680	BOL-B BOL-B 2160	BOL-B BOL-B 2160	BOL-D BOL-D 1680	BOL-B BOL-B 2160	BOL-E BOL-E 1440	BOL-D BOL-D 1680	BOL-B BOL-B 2160	BOL-D BOL-D 1680	BOL-B BOL-B 2160	BOL-B BOL-B 2160	BOL-D BOL-D 1680
Sector 11	BOL-D BOL-D 1680	BOL-B BOL-B 2160	BOL-B BOL-B 2160	BOL-D BOL-D 1680	BOL-B BOL-B 2160	BOL-D BOL-D 1680	BOL-D BOL-D 1680	BOL-B BOL-B 2160	BOL-D BOL-D 1680	BOL-B BOL-B 2160	BOL-B BOL-B 2160	BOL-D BOL-D 1680
Sector 13	BOL-D BOL-D 1680	BOL-B BOL-B 2160	BOL-B BOL-B 2160	BOL-E BOL-E 1440	BOL-E BOL-E 1440	BOL-D BOL-D 1680	BOL-B BOL-B 2160	BOL-E BOL-E 1440	BOL-E BOL-E 1440	BOL-B BOL-B 2160	BOL-B BOL-B 2160	BOL-D BOL-D 1680
Sector 15	BOL-D BOL-D 1680	BOL-B BOL-B 2160	BOL-B BOL-B 2160	BOL-D BOL-D 1680	BOL-B BOL-B 2160	BOL-D BOL-D 1680	BOL-D BOL-D 1680	BOL-B BOL-B 2160	BOL-D BOL-D 1680	BOL-B BOL-B 2160	BOL-B BOL-B 2160	BOL-D BOL-D 1680

Figure 13: Assignment of the BOL RPC units to the muon stations.